Pore-Level Examination of Gel Destruction During Oil Flow

R.S. Seright, SPE, New Mexico Petroleum Recovery Research Center; **W. Brent Lindquist,** SPE, and **Rong Cai,** Stony Brook University

Summary

Pore-scale X-ray computed microtomography (XMT) images were obtained at a variety of oil (hexadecane) throughput values after gel placement in cores [involving a pore-filling Cr(III)-acetate-hydrolyzed polyacrylamide (HPAM) gel]. For each pore in our image volume, we followed oil and water saturations as a function of oil throughput. These studies were performed both in water-wet Berea sandstone and in hydrophobic porous polyethylene cores. In hydrophobic porous polyethylene, oil saturations increased and gel was destroyed (presumably dehydrated) quite quickly in the smallest pores. Also, oil saturations increased and gel was destroyed quickly in the largest pores. In contrast, oil saturations rose much more gradually for the most common or intermediate-size pores (around 10^{-4} mm^3). The minimum in oil saturation vs. pore size may result from a balance between gel dehydration by oil film growth vs. gel extrusion.

In contrast, in water-wet Berea sandstone, increases in oil saturation occurred evenly over all pore sizes (10^{-6} to 0.02 mm^3) for all oil throughput values. Consistent with imbibition and drainage studies performed before gel placement, oil apparently had equal access to Berea pores of all sizes and, thus, uniformly dehydrated gel in pores of all sizes. Gel extrusion did not appear to be significant in the Berea pores.

Introduction

An ability of gels to reduce permeability to water much more than that to oil is critical for successful applications of gel treatments in production wells if hydrocarbon zones are not protected during gel placement (Liang et al. 1993; Sydansk and Seright 2007). If gelant penetrates into an oil zone and gel forms, some time will be required before the oil penetrates through the gel bank and significant restoration of permeability to oil can occur (Seright 2006, 2009). The dependence of permeability on oil throughput determines how long it takes for a production well to restore productivity after a gel treatment.

In our previous work, XMT was used to establish why pore-filling Cr(III)-acetate-HPAM gels reduced permeability to water much more than to oil. Our results suggest that permeability to water was reduced to low values because water must flow through gel itself, whereas oil pressing on the gel in a porous rock forced pathways by dehydration—leading to relatively high permeability to oil. Those studies involved obtaining 3D pore-level X-ray images at the saturation endpoints [e.g., after forcing 20 pore volumes (PV) of oil or water through the core following gel placement]. To understand the rate of restoration of permeability to oil after a gel treatment, we are interested in how the gel dehydration process progresses as a function of oil throughput. This study uses XMT to understand the throughput dependence of oil permeability after gel placement.

The XMT Method

In this paper, we describe imaging experiments using high-resolution computed X-ray microtomography to compare the oil and water pathways and fluid distributions at various stages before and after gel placement in cores. We used the ExxonMobil Beamline X2-B at the National Synchrotron Light Source (Flannery et al. 1987; Dunsmuir et al. 1991; Seright et al. 2002, 2003, 2006). To avoid end effects, imaging was performed within a 6.5-mm-diameter, 3.25-mm-long segment of each core centrally located along its 30-mm length. Depending on the experiment, voxel resolution was from 4.1 to 4.93 μm and the total image volume was from 29 to 50.5 mm^3. Image analysis typically focused on a 450 × 450 × 475 voxel region of each image. The 3DMA-Rock software package was used to analyze the image sequences. Its segmentation algorithm, based upon indicator kriging, was used to segregate grain/void space in the first image in each sequence and to separate oil/water phases within the pore space in each subsequent image. The method can distinguish between rock, water, and oil. However, it cannot distinguish between water and gel (which is composed of >98% water). Details of these procedures and analytical methods can be found in our previous references (Lindquist et al. 1996; Seright et al. 2006; Prodanovic et al. 2006, 2007).

Core Properties

We used Berea sandstone and porous polyethylene as core materials (Seright et al. 2006). The Berea cores had permeabilities of 0.3 to 0.5 darcies and a porosity of 0.2. The polyethylene cores had permeabilities of 8 to 10 darcies and a porosity of 0.4. Wettability tests produced Amott-Harvey indexes of 0.7 for the brine (1% NaCl, 0.1% $CaCl_2$)/oil (hexadecane)/Berea sandstone system and –0.8 for the brine/oil/porous polyethylene system—confirming the water-wet character of Berea sandstone and the hydrophobic character of porous polyethylene. On the basis of XMT analysis, the two porous media have very similar pore size distributions (Seright et al. 2006, 2008). **Table 1** summarizes the core properties (Seright et al. 2002, 2006; Prodanovic et al. 2006, 2007). The average pore size was 0.00052 mm^3 for polyethylene and 0.00035 mm^3 for Berea. If the pores were spherical (which they are not), the average pore radius would be 50 μm for polyethylene and 44 μm for Berea. The average pore throat area was 1,400 μm^2 for Berea sandstone and 1,630 μm^2 for porous polyethylene. The average pore throat radius (assuming circular throat areas) was 11 μm for Berea and 11.4 μm for polyethylene. The aspect ratio can be defined as the effective pore radius divided by the effective throat radius. (The effective pore radius computed is for a sphere with a volume equivalent to that measured for the pore. The effective throat radius computed is for a circle with an area equivalent to that measured for the throat.) As shown in Table 1, the average aspect ratio was approximately 4 for both Berea and polyethylene. The average coordination number was 4 for Berea sandstone and 6 for porous polyethylene (Seright et al. 2002). (The coordination number is the number of exits from a pore.) More detailed descriptions of the microscopic core properties can be found in Seright et al. 2008 and in the other references in this paragraph.

Imbibition and Drainage Before Gel Placement

In previous work (Seright et al. 2002, 2003, 2006; Prodanovic et al. 2006, 2007), we obtained XMT images and analysis for Berea and polyethyelene cores at endpoint saturations of oil (hexadecane) and brine (with 1% NaCl, 0.1% $CaCl_2$) before gel placement. Comparison between drainage and imbibition in both porous media before gel placement provided an interesting insight into conventional

This paper (SPE 112976) was accepted for presentation at the SPE/DOE Symposium on Improved Oil Recovery, Tulsa, 20–23 April 2008, and revised for publication. Original manuscript received for review 8 February 2008. Revised manuscript received for review 26 June 2008. Paper peer approved 21 August 2008.

TABLE 1—SUMMARY OF CORE PROPERTIES		
Property	Berea sandstone	Porous polyethylene
Wettability	Water-wet	Oil-wet
Permeability	0.47 darcies	8.8 darcies
Porosity	0.2	0.4
Average pore radius	44 μm	50 μm
Average throat radius	11 μm	11.4 μm
Average body/throat aspect ratio	4.0	4.4
Average coordination number	4	6

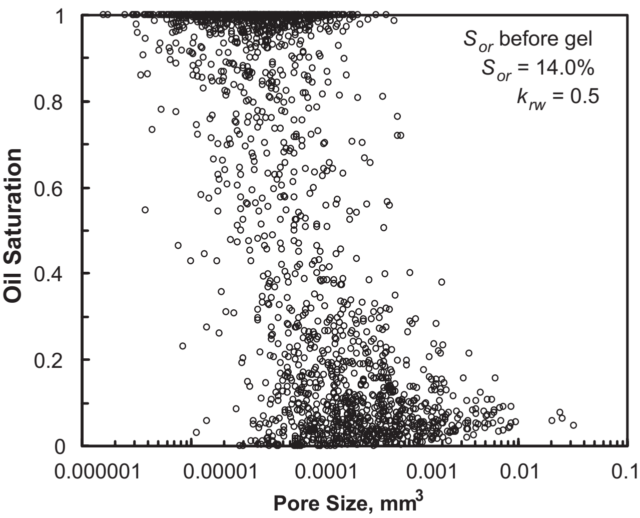

Fig. 1—Polyethylene at S_{or} before gel.

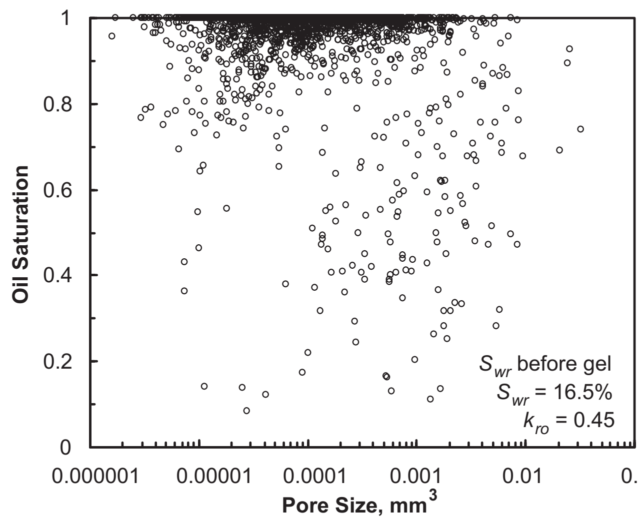

Fig. 2—Polyethylene at S_{wr} before gel.

wisdom. When a wetting phase drains from a porous medium, conventional wisdom argues that the smallest pores should retain the highest wetting-phase saturation. This expectation is consistent with our findings after water injection into (oil drainage from) oil-wet porous polyethylene **(Fig. 1).** After the first drainage displacement (to residual oil saturation or S_{or}), oil saturation in the imaged region of the polyethylene core was 14%. As expected, the average oil (wetting phase) saturation in the smallest detected pores was more than 80% while the medium to large pores were more likely to be filled with water. During a second cycle of oil drainage (i.e., a second waterflood to drive the core to S_{or} after an intervening oil flood), most large pores again filled almost completely with water, while most small pores retained high oil saturations (Seright et al. 2006). When oil was injected to drive the core to residual water saturation, S_{wr}, water was displaced from most medium to large pores so that most pores ended with nearly 100% oil saturation **(Fig. 2).** Thus, consistent with conventional wisdom, the wetting phase was largely immobile in small polyethylene pores.

In Berea sandstone, at connate water saturation (S_{wr}) before gel placement, S_w in the imaged region was 16%. The water saturations at S_{wr} are plotted in **Fig. 3** for each of the pores in the Berea sample volume. At S_{wr}, 54.5% of the pores had $S_w < 5\%$; water saturations near zero were common for pores in most size ranges. Water saturations in the smallest pores were scattered over the entire range from 0 to 100%—just as in most other size ranges (Seright et al. 2006). A calculation using the Young-LaPlace equation confirmed that oil should readily be able to enter the smallest pores (~10^{-5} mm^3) in our Berea cores (Seright et al. 2002).

On first consideration, this finding appears to contradict the expectation that the water saturations approach 100% in the smallest pores of a water-wet porous medium. The work of Dullien et al. (1989) helps to explain the behavior that we see in Berea and why it deviates from that in polyethylene. Berea pores are typically coated with kaolinite that significantly increases the surface roughness of the pore walls. In contrast, the pore walls in polyethylene are quite smooth (Seright et al. 2006). At S_{or}, after oil drainage from the smooth polyethylene pore walls, an extremely thin (nanometer scale) oil film may have coated most pore walls (or possibly, no film may remain). At S_{wr} in water-wet Berea, the rough clay coating made the effective thickness of the water film much greater than for any oil film in porous polyethylene. With a thicker effective wetting film, water drained fairly efficiently from the smallest detected Berea pores when oil was injected—thus allowing the smallest detected pores to reach water saturations comparable to those in larger pores. In contrast, when water was injected into porous polyethylene, oil usually became hydraulically isolated in the smallest detected pores because any remaining wetting film was too thin to efficiently drain oil. Consequently, high oil saturations were usually seen in the smallest detected polyethylene pores. The

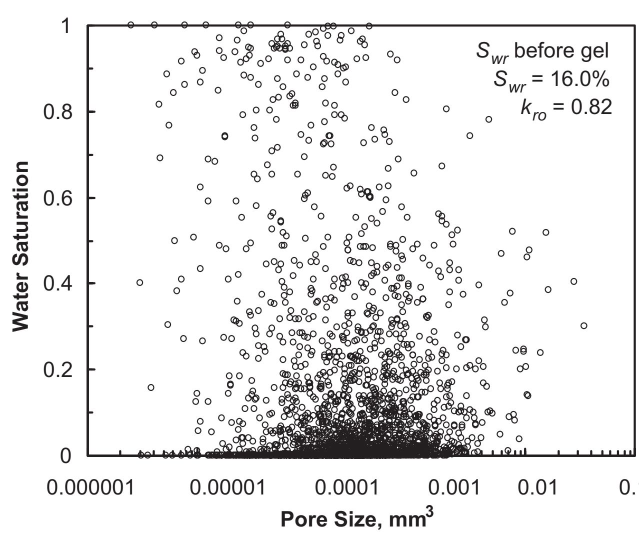

Fig. 3—Berea at S_{wr} before gel.

important message here is that, for the pore sizes involved with our porous media, access to pores (through effective films) is at least as important in determining residual saturations as capillary pressure, interfacial tension, or applied pressure gradient (Seright et al. 2006, 2008).

We also studied oil and water saturations in pores as a function of water and oil throughput in porous polyethylene cores (Prodanović et al. 2006). For any given throughput, the residual wetting-phase (oil) saturations in these pores did not change much during either drainage (water injection) or imbibition (subsequent oil injection); specifically, less than 10% of these pores experienced a significant saturation change. In contrast, 60–70% of the residual nonwetting phase (water) moves during both imbibition and drainage (Prodanović et al. 2006, Table 7). These studies also showed that, during drainage (water injection into porous polyethylene), the nonwetting phase (water) filled the largest pores first. During imbibition (oil injection), water leaves the largest pores last. For cases where fractional flow was fixed, water saturations tended to decrease with decreased pore size.

Current Mechanistic View for Disproportionate Permeability Reduction by Pore-Filling Gels

This section summarizes our current view of the mechanism for disproportionate permeability reduction for pore-filling gels such as Cr(III)-acetate-HPAM. Immediately after placement and gelation, the water-based gel occupies all of the aqueous pore space. Residual oil may be trapped in pore centers in water-wet rock, such as Berea. In oil-wet porous media (e.g., porous polyethylene), low mobility "residual oil" may coat pore walls. With either wetting condition, if water or brine is injected after gel placement, it must flow through the gel itself. Because the inherent permeability to water is in the microdarcy range for flow through the gel, a very large permeability reduction is observed (Seright 1993). For rock with an initial permeability (before gel) of approximately 1 darcy, the water residual resistance factor can be greater than 10,000. Thus, the gel can greatly reduce flow from gel-invaded water zones.

Oil is typically the first fluid that contacts the gel-treated region when a well is returned to production. We found that oil flow reduces the pore volume occupied by gel. This volume reduction created pathways for oil flow, thus restoring an important level of permeability to oil.

When oil is injected, how does a reduction in gel volume occur? Several possibilities come to mind, including oil (a) ripping through the gel, (b) concentrating or dehydrating the gel, (c) mobilizing or extruding the gel, or (d) chemically destroying the gel. As our oil (hexadecane) was not reactive with any of the gel, brine, or rock components, possibility (d), chemical destruction of the gel, does not seem likely. Our analysis supports the dehydration mechanism in Berea sandstone over the ripping or gel mobilization mechanisms (Seright et al. 2006). In particular, the apparent reduction in gel saturation during oil injection was insensitive to pore size in Berea and was greatest in small pores in porous polyethylene. If ripping or gel mobilization were the dominant mechanisms, losses in gel volume should have been greatest in the largest pores. To explain, if gel failure (i.e., ripping or gel extrusion) occurred at a gel/rock interface or within the gel, force balance analysis suggests that the pressure gradient for gel failure should be inversely proportional to the pore radius (Zaitoun et al. 1998; Liu and Seright 2001). Thus, for a given applied pressure gradient, gel failure should occur dominantly in larger pores. Because this did not occur, our results argue against the ripping or gel mobilization mechanisms. In contrast, the observed XMT results could be consistent with the dehydration mechanism. With a fixed pressure gradient applied through the porous medium, gel in all pores could be "squeezed" or dehydrated to the same extent, regardless of pore size. In very permeable sand packs, data from other researchers supports ripping or extrusion mechanisms for creating oil pathways (Seright et al. 2006; Nguyen et al. 2006).

Imbibition and Drainage as a Function of Throughput After Gel Placement

Our XMT previous studies that were performed after gel placement obtained images at the saturation endpoints—for example, after forcing 20 pore volumes of oil or water through the core after gel placement (Seright et al. 2002, 2003, 2006). The dependence of oil permeability on oil throughput determines how long it takes for a production well to "clean up" or restore productivity after a gel treatment (Seright 2006, 2009). Consequently, we were interested in how the gel dehydration process progresses as a function of oil throughput—not just at saturation endpoints as in our previous XMT studies performed post gel placement (Seright et al. 2002, 2003, 2006). We were particularly interested in whether oil paths develop preferentially in large vs. small pores. To answer this question, we saturated a polyethylene core (8 darcy original permeability, 40% porosity) and a Berea sandstone core (328 md original permeability, 20% porosity) with a Cr(III)-acetate-HPAM gelant and allowed the gel to form. This gel contained 0.5% Ciba Alcoflood 935 HPAM, 0.0417% Cr(III) acetate, 1% NaCl, and 0.1% $CaCl_2$. During placement, the gelant viscosity was 20 cp. The oil was hexadecane doped with 15% bromohexadecane (to enhance X-ray attenuation for the oil phase). The oil viscosity was 3 cp. The pressure gradient during oil injection was always less than 10 psi/ft. During oil injection, the rate was 0.1 PV/min for total injection values from 0.1 to 1 PV; 1 PV/min for total injection volumes from 2 to 10 PV; and 10 PV/min for total injection volumes greater than 10 PV. As demonstrated in Seright 2009, restoration of oil permeability correlates strongly with oil throughput. For a given oil throughput, the level of oil permeability restored is not sensitive to injection rate or pressure gradient (up to a point where high pressure gradients induce gel destruction by extrusion—typically > 50 psi/ft). Our cores were 3 cm long and 0.65 cm in diameter. All experiments were performed at room temperature.

For the current experiments, residual oil was not present during placement of our gelant. Of course, residual oil will be present for many field applications. Results where oil was present before gelant placement can be found in Seright 2006 and 2009 (for non-XMT studies of restoration of oil permeability vs. oil throughput) and in Seright et al. 2006 (for XMT studies at the saturation endpoints). The presence of residual oil at the time of gelant placement can increase the initial permeability during the first oil or water injection after gel placement (Seright 2009). However, other trends and conclusions are quite similar regardless of whether residual oil is present at the time of gel placement (Seright 2006, 2009; Seright et al. 2006).

Average Saturations in the XMT Image Volume. For our current experiments, **Fig. 4** plots the average saturation in the XMT image volume as a function of PV of oil injected. One surprising aspect of the results was that the average saturation from the XMT data was noticeably greater than expected from the oil throughput

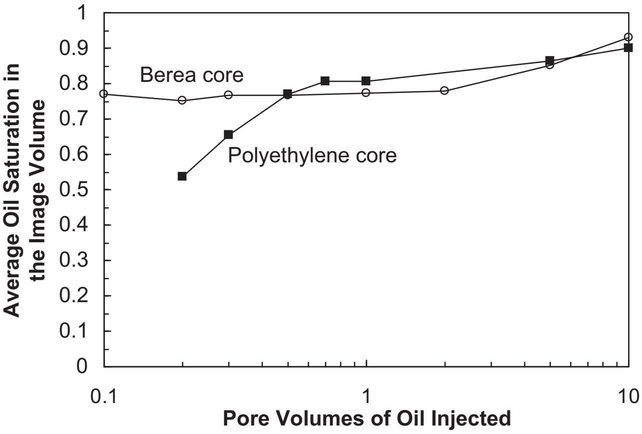

Fig. 4—Average oil saturations in the image volumes vs. oil throughput.

data. In the polyethylene core, the average oil saturation in the image volume reached 54% after injecting only 0.2 PV of oil. In the Berea sandstone core, the average oil saturation in the image volume reached 77% after injecting only 0.1 PV of oil. On first consideration, these findings do not seem possible. One would expect that the average oil saturation in the core could not exceed 10% after injecting 0.1 PV of oil and 20% after injecting 0.2 PV of oil. However, remember that the saturations were measured in the image volume. The image volume was only 12 mm^3 in the center of a 1,300 mm^3 core. The mobility ratio was extremely high during oil flow through the gel. A finger of oil could reach a given location within the core with a very small throughput. Consequently, it is quite possible that the image volume may be flooded to high oil saturation at an earlier time than the average for the core. By the same logic, it is possible that the oil fingers might completely miss the image volume, so that oil saturations remain low until very high throughput values. Thus, some degree of "luck" or random chance led to the particular saturations levels seen in Fig. 4. Nonetheless, within a given image volume, the distribution of oil in small, medium, and large pores is of interest.

XMT Results for the Polyethylene Core. The distribution of oil saturations as a function of pore size and oil throughput in the image volume of the polyethylene core is shown in **Fig. 5.** For all throughput values, a minimum in oil saturation was observed for pore sizes of approximately 5×10^{-5}–10^{-4} mm^3. (The oil saturation minimum moved to slightly lower pore sizes with increased oil throughput—from 6×10^{-5} mm^3 at 0.2 PV to 4×10^{-5} mm^3 at 10 PV.) The smallest polyethylene pores (10^{-6}–10^{-5} mm^3) filled rapidly with oil. Oil saturations jumped to almost 60% in these pores after injecting only 0.2 PV of oil. We speculate that the hydrophobic polyethylene pore walls provided an effective conduit to imbibe oil through the porous medium. Presumably, growth of an oil film on the pore walls led to compression of the gel. This compression forced a small amount of water to flow through the gel structure to the outlet end of the core (i.e., gel dehydration). Also presumably, this slight loss of water caused a small increase in concentration of polymer within the gel (Seright et al. 2006).

In contrast, oil saturations rose much more gradually for the most common or intermediate-sized pores. For pores with sizes of approximately 5×10^{-5} mm^3, oil saturations were 0.24 at 0.2 PV, 0.38 at 1 PV, and 0.64 at 5 PV. Conceivably, the slower rise in oil saturations could be responsible for the gradual increase in k_o that was reported by Seright (2006, 2009). There are so many pores within the size range of approximately 5×10^{-5}–10^{-4} mm^3 that the oil must flow through these pores to get through the core. Thus, these pores provide the critical resistance that determines the overall permeability.

The largest pores also filled quite rapidly with oil. For pores larger than 0.0063 mm^3 (accounting for 61% of the total pore space in the image volume), the oil saturation was greater than 90% after injecting only 0.3 PV. Although it is possible that gel dehydration was responsible for the gains in oil saturation in these pores, we are inclined to believe that ripping or gel extrusion were more likely the responsible mechanisms. We note that, in sand packs with permeabilities comparable to our polyethylene core, data from the University of Kansas supports ripping or extrusion mechanisms for creating oil pathways (Seright et al. 2006; Nguyen et al. 2006). The hydrophobic polyethylene surface probably allowed a film of oil to penetrate into all pores, where it could act as a lubrication layer to facilitate gel extrusion from the pore. Gel extrusion most likely occurs in the largest pores, thus explaining why the oil saturation in Fig. 5 increased with increased pore size above 10^{-4} mm^3. No gel was physically observed extruding from the cores. However, it is quite possible that any extruded gel was too small and too dilute to notice visually.

Consequently, the minimum in oil saturation vs. pore size in Fig. 5 may result from a balance between gel dehydration by oil film growth vs. gel extrusion. Presumably, the oil film thickness is about the same on all polyethylene surfaces. However, because the ratio of film thickness to pore or throat size increases with decreased pore size, gel dehydration occurs faster and more effectively in the smallest polyethylene pores, causing oil saturation to decrease with increased pore size (left side of Fig. 5). This effect loses significance for pore sizes greater than 10^{-4} mm^3, where gel extrusion from the pore becomes more likely—explaining why oil saturation increased with increased pore size for the right side of Fig. 5.

XMT Results for the Berea Sandstone Core. The distribution of oil saturations as a function of pore size and oil throughput in Berea sandstone are shown in **Fig. 6.** For any given oil throughput, oil saturation was fairly independent of pore size. Why did the smallest Berea pores not experience large increases in oil saturation, as was observed in the polyethylene core? Presumably, the answer is that the water-wet Berea rock had no propensity to imbibe oil, so no oil film formed and grew as suggested for the hydrophobic polyethylene. Why did the largest Berea pores not show large increases in oil saturation, as was observed in the polyethylene core? The porosity of the Berea rock was about half that for polyethylene. Perhaps the ripping and extrusion mechanisms were more prevalent in the high-porosity polyethylene. Also, in polyethylene, perhaps the oil film promoted (through lubrication) gel extrusion from the largest pores. In Berea sandstone, this oil film probably was not present. Instead consistent with imbibition and drainage studies performed before gel placement in Berea sandstone, oil apparently had equal access to Berea pores of all sizes, and thus uniformly dehydrated gel in pores of all sizes. Gel extrusion did not appear to be significant in the Berea pores.

Interestingly, the average oil saturation jumped to approximately 0.75 in Berea after injection of only 0.1 PV of oil (Fig. 4). In contrast, in porous polyethylene, an oil saturation of 0.75 had not been reached in the mid-sized pores until injection of 10 PV of

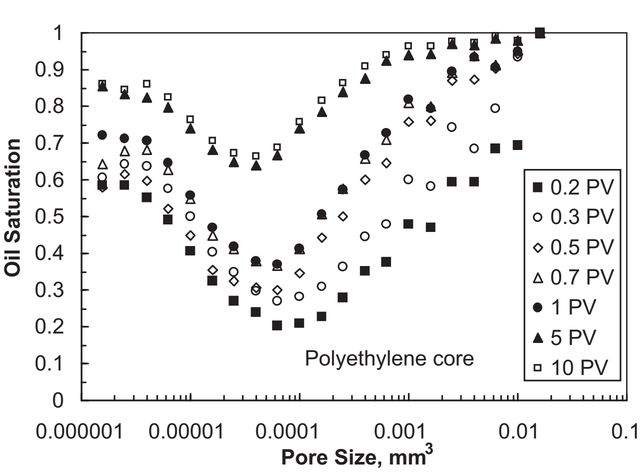

Fig. 5—Oil saturation vs. pore size and oil throughput: polyethylene core.

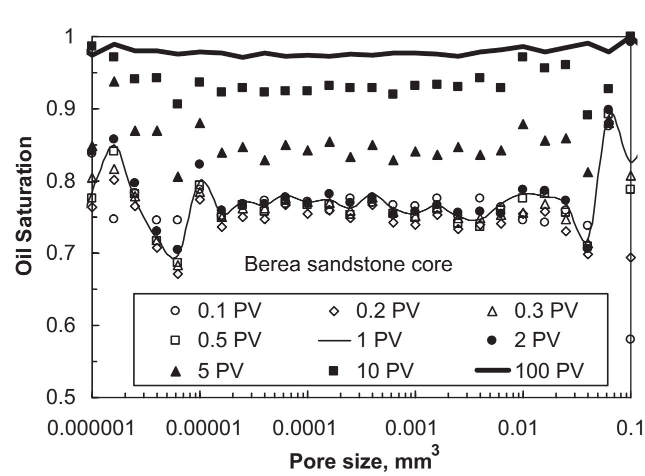

Fig. 6—Oil saturation vs. pore size and oil throughput: Berea core.

oil (Fig. 5). The rate of increase in oil permeability was roughly the same for the two porous media (Seright et al. 2008). The rapid jump in oil saturation in Berea between 0 and 0.1 PV may have occurred simply because the oil finger fortuitously swept the imaged volume. In contrast, in polyethylene, the small image volume apparently was swept less rapidly (see the left side of Fig. 4).

The unfavorable displacement and the resulting wormholing/fingering effect have implications for the ultimate utility of our XMT results. In particular, although our XMT studies give insights into oil penetration through gel on a microscopic level, the results cannot be directly scaled to predict oil penetration rate on the meter or field scales. For the latter activity, we must still rely on empirical observations discussed during our other work (Seright 2006, 2009).

Conclusions

To understand gel destruction on a microscopic scale, pore-scale XMT images were obtained at a variety of oil (hexadecane) throughput values after gel placement [involving a pore-filling Cr(III)-acetate-HPAM gel]. For each pore in our image volume, we followed oil and water/gel saturations as a function of oil throughput. These studies were performed both in water-wet Berea sandstone and in hydrophobic porous polyethylene.

- In hydrophobic porous polyethylene, oil saturations increased and gel was destroyed (presumably dehydrated) quite quickly in the smallest pores (10^{-6} mm^3). Also, oil saturations increased and gel was destroyed quickly in the largest pores (<0.005 mm^3). In contrast, oil saturations rose much more gradually for the most common or intermediate-sized pores (approximately 5×10^{-5}–10^{-4} mm^3, the peak in the pore size distribution). The minimum in oil saturation vs. pore size may result from a balance between gel dehydration by oil film growth vs. gel extrusion.
- In contrast, in water-wet Berea sandstone, increases in oil saturation occurred evenly over all pore sizes (10^{-6} to 0.02 mm^3) for all oil throughput values. Consistent with imbibition and drainage studies performed before gel placement, oil apparently had equal access to Berea pores of all sizes, and, thus, uniformly dehydrated gel in pores of all sizes. Gel extrusion did not appear to be significant in the Berea pores.
- Although our XMT studies give insights into oil penetration through gel on a microscopic level, the results cannot be directly scaled to predict oil penetration rate on the meter or field scales. For the latter activity, we must still rely on empirical observations discusses during our other work (Seright 2006, 2009).

Nomenclature

k = permeability, darcy [μm^2]
k_o = permeability to oil, darcy [μm^2]
k_{ro} = relative permeability to oil
k_{rw} = relative permeability to water
S_o = oil saturation
S_{or} = residual oil saturation
S_w = water saturation
S_{wr} = residual water saturation
ϕ = porosity

Acknowledgments

We gratefully acknowledge ConocoPhillips, ExxonMobil, and Marathon for financial support of this work. This research was carried out in part at the National Synchrotron Light Source, Brookhaven National Laboratory, which is supported by the US Department of Energy, Division of Materials Sciences and Division of Chemical Sciences. We are also grateful to John Dunsmuir and ExxonMobil for the use of Beamline X2-B.

References

Dullien, F.A.L., Zarcone, C., Macdonald, I.F., Collins, A., and Bochard, R.D.E. 1989. The effects of surface roughness on the capillary pressure curves and the heights of capillary rise in glass bead packs. *Journal of Colloid and Interface Science* **127** (2): 362–372. DOI: 10.1016/0021-9797(89)90042-8.

Dunsmuir, J.H., Ferguson, S.R., D'Amico, K.L., and Stokes, J.P. 1991. X-Ray Microtomography: A New Tool for the Characterization of Porous Media. Paper SPE 22860 presented at the SPE Annual Technical Conference and Exhibition, Dallas, 6–9 October. DOI: 10.2118/22860-MS.

Flannery, B.P., Deckman, H.W., Roberge, W.G., and D'Amico, K.L. 1987. Three-Dimensional X-Ray Microtomography. *Science* **237** (4821): 1439–1444. DOI: 10.1126/science.237.4821.1439.

Liang, J.-T., Lee, R.L., and Seright, R.S. 1993. Gel Placement in Production Wells. *SPE Prod & Fac* **8** (4): 276–284; *Trans.,* AIME, **295**. SPE-20211-PA. DOI: 10.2118/20211-PA.

Lindquist, W.B., Lee, S.-M., Coker, D.A., Jones, K.W., and Spanne, P. 1996. Medial axis analysis of void structure in three-dimensional tomographic images of porous media. *J. Geophys. Res.* **101** (B4): 8297–8310. DOI: 10.1029/95JB03039.

Liu, J. and Seright, R.S. 2001. Rheology of Gels Used for Conformance Control in Fractures. *SPE J.* **6** (2): 120–125. SPE-70810-PA. DOI: 10.2118/70810-PA.

Nguyen, T.Q., Green, D.W., Willhite, G.P., and McCool, C.S. 2006. Effects of Gelant Composition and Pressure Gradients of Water and Oil on Disproportionate Permeability Reduction of Sandpacks Treated With Polyacrylamide-Chromium Acetate Gels. *SPE J.* 11 (2): 145–157. SPE-89404-PA. DOI: 10.2118/89404-PA.

Prodanović, M., Lindquist, W.B., and Seright, R.S. 2006. Porous structure and fluid partitioning in polyethylene cores from 3D X-ray microtomographic imaging. *Journal of Colloid and Interface Science* **298** (1): 282–297. DOI: 10.1016/j.jcis.2005.11.053.

Prodanović, M., Lindquist, W.B., and Seright, R.S. 2007. 3D image-based characterization of fluid displacement in a Berea core. *Advances in Water Resources* **30** (2): 214–226. DOI: 10.1016/j.advwatres.2005.05.015.

Seright, R.S, Liang J., Lindquist, W.B., and Dunsmuir, J.H. 2002. Characterizing Disproportionate Permeability Reduction Using Synchrotron X-Ray Computed Microtomography. *SPE Res Eval & Eng* **5** (5): 355–364. SPE-79717-PA. DOI: 10.2118/79717-PA.

Seright, R.S. 1993. Effect of rock permeability on gel performance in fluid-diversion applications. *In Situ* **17** (4): 363–386.

Seright, R.S. 2006. Clean Up of Oil Zones After a Gel Treatment. *SPE Prod & Oper* **21** (2): 237–244. SPE-92772-PA. DOI: 10.2118/92772-PA.

Seright, R.S. 2009. Disproportionate Permeability Reduction With Pore-Filling Gels. *SPE J.* **14**(1): 5–13. SPE-99443-PA. DOI: 10.2118/99443-PA.

Seright, R.S., Liang, J., Lindquist, W.B., and Dunsmuir, J.H. 2003. Use of X-ray computed microtomography to understand why gels reduce permeability to water more than that to oil. *J. Pet. Sci. Eng.* **39** (3–4): 217–230. DOI: 10.1016/S0920-4105(03)00064-0.

Seright, R.S., Lindquist, W.B, and Cai, R. 2008. Understanding the Rate of Clean Up for Oil Zones After a Gel Treatment. Paper SPE 112976 presented at the SPE/DOE Symposium on Improved Oil Recovery, Tulsa, 20–23 April. DOI: 10.2118/112976-MS.

Seright, R.S., Prodanovic, M., and Lindquist, W.B. 2006. X-Ray Computed Microtomography Studies of Fluid Partitioning in Drainage and Imbibition Before and After Gel Placement. *SPE J.* **11** (2): 159–170. SPE-89393-PA. DOI: 10.2118/89393-PA.

Sydansk, R.D. and Seright, R.S. 2007. When and Where Relative Permeability Modification Water-Shutoff Treatments Can Be Successfully Applied. SPE Prod & Oper **22** (2): 236–247. SPE-99371-PA. DOI: 10.2118/99371-PA.

Zaitoun, A., Bertin, H., and Lasseux, D. 1998. Two-Phase Flow Property Modifications by Polymer Adsorption. Paper SPE 39631 presented at the SPE/DOE Improved Oil Recovery Symposium, Tulsa, 19–22 April. DOI: 10.2118/39631-MS.

Randy Seright is a senior engineer at the New Mexico Petroleum Recovery Research Center at New Mexico Tech in Socorro, New Mexico, where he has worked since 1987. email: randy@prrc.nmt.edu. He holds a PhD degree in chemical engineering from the University of Wisconsin at Madison. Seright received the SPE/DOE IOR Pioneer Award in 2008. **W. Brent Lindquist** is a professor of computational applied mathematics in the Department of Applied Mathematics and Statistics and deputy provost at Stony Brook University. email: lindquis@ams.sunysb.edu. He holds a PhD in theoretical physics from Cornell University. His research interest is flow in porous media. Currently, he is concentrating on the problem of up-scaling chemical reaction rates. **Rong Cai** is a graduate student working on her PhD in applied mathematics and statistics at Stony Brook University. email: rongcai@ams.sunysb.edu.